

Noise Evolution Along Optically Amplified Links in Presence of Nonlinear Parametric Gain

Michele Norgia, *Student Member, IEEE*, Guido Giuliani, *Member, IEEE*,
and Silvano Donati, *Senior Member, IEEE, Member, OSA*

Abstract—With a semiclassical model of the optical amplifier, we calculate the evolution of noise along optically amplified lines in presence of nonlinear interaction between signal and amplified spontaneous emission, amplifiers saturation, fiber dispersion and vacuum field fluctuations associated with attenuation of the fiber. The noise figure (NF) is calculated for two representative cases of long and short-distance links with different numbers of optical amplifiers and for several fiber dispersions. Results indicate that the optimum number of optical amplifiers is limited by the increase of nonlinear effects with signal power.

Index Terms—Amplifier noise, communication system nonlinearities, nonlinear wave propagation, optical amplifiers, optical fiber amplifiers, optical fiber communication, optical noise, spontaneous emission.

I. INTRODUCTION

RECENTLY, considerable interest has been attracted by the evaluation of optically amplified fiber links, in which noise and saturation of the optical amplifier (OA in the following) [1]–[4] as well as fiber nonlinearities [5] interact to determine the evolution of signal-to-noise ratio SNR along the line.

In particular, link performances are affected by four-wave mixing (FWM), modulation instability (MI), and parametric gain (PG). Their impact on amplifier noise has been studied theoretically [6]–[9] and experimentally [10]–[11] with reference to return-to-zero (RZ) and nonreturn-to-zero (NRZ) systems [12].

To calculate the evolution of the spectral distribution of a probe signal along an optically amplified line, we describe the OA by means of a recently introduced semiclassical noise-model [1], in which we now also include the effects of PG on the amplified spontaneous emission (ASE). To be specific, we focus on the erbium-doped fiber amplifiers (EDFA's) and take into account the effective spectral gain shape and the saturation, treating cascaded amplifiers in a self-consistent description.

We substantiate the results through two reference cases: 1) a long-haul transmission link (e.g., 2500 km) and 2) a medium-length link (120 km), representative of intercity trunks. In both cases, we study the noise figure (NF) evolution with OA's number and trunk length, with dispersion as a parameter.

Results already known in literature are confirmed by our quite different model, that has the attractive feature of not requiring any *ad hoc* hypothesis. Also, we find that the optimum OA's number is mostly dependent on nonlinear effects rather than by the increase of ASE.

In Section II, we summarize the models of OA noise, fiber and nonlinearities used in the calculations. In Section III, we report the results of ASE evolution in links without nonlinearities, in Section IV a theoretical description of the Parametric Gain, and in Section V the results of long- and short-length links with nonlinearities and dispersion.

II. MODELS OF THE BLOCKS

A. OA Noise Model

As in [1], we model the OA as a four-port device described by the following transfer matrix for the optical field:

$$\begin{bmatrix} B \\ B' \end{bmatrix} = \begin{bmatrix} \sqrt{G} & i\sqrt{G-1} \\ i\sqrt{G-1} & \sqrt{G} \end{bmatrix} \begin{bmatrix} A \\ A' \end{bmatrix} \quad (1)$$

where G is the amplifier (power) gain, A and A' are the input signal and idler fields, B, B' are the output signal and idler fields. This model is rigorous from quantum-mechanics point of view [1], and can be interpreted as if the OA were a beamsplitter with a fictitious $G > 1$ factor of power transmittance. The unused input port, a direct consequence of Heisenberg uncertainty principle, is opened to a vacuum field mode ΔE_{VAC} at signal frequency ν , with a zero-mean white gaussian noise and a bilateral spectral density $S_{\text{VAC}} = \frac{1}{4}h\nu$, as directly coming from second quantization.

Incomplete inversion of the amplifying medium, i.e., the $N_{\text{sp}} > 1$ spontaneous emission coefficient, is taken into account by adding another beamsplitter of field transmission $\sqrt{N_{\text{sp}}}$ before the idler input port [see Fig. 1(a)].

The model has the block-scheme counterpart shown in Fig. 1(b), from which we readily find the output-noise field power-spectral density as

$$S_{\text{OUT}} = GS_{\text{IN}} + (2N_{\text{sp}} - 1)(G - 1)S_{\text{VAC}} \quad (2)$$

where S_{IN} is the power spectral density of the input field (accounting for excess noise, as brought by the ASE of preceding OA's). The spectral density of the normalized photocurrent S_i detected by a photodiode is calculated in the Appendix as function of the total radiation spectral density,

Manuscript received October 12, 1998; revised June 23, 1999. This work was supported under a Madess II Contract.

The authors are with the Dipartimento di Elettronica, University of Pavia, Pavia I-27100 Italy.

Publisher Item Identifier S 0733-8724(99)08014-7.

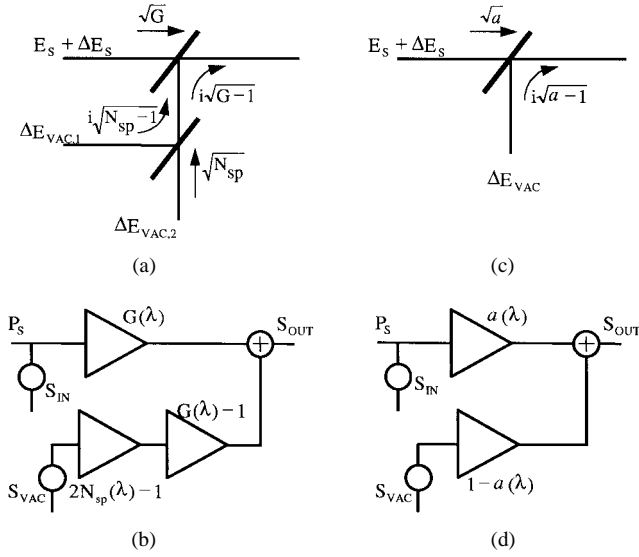


Fig. 1. (a) The OA is modeled as a beamsplitter with transmittance G ; the incomplete inversion is taken into account by vacuum fields amplification factor N_{sp} . (b) OA noise equivalent circuit. (c) The optical fiber is modeled as a beamsplitter with transmittance a . (d) Fiber noise equivalent circuit.

written as the sum of signal s and noise a ($S_{rad} = S_s + S_a$)

$$S_i(f) = \left[\int_{-\infty}^{+\infty} (S_s(f) + S_a(f) - S_{VAC}(f)) df \right]^2 \delta(f) + 2S_a(f) \otimes S_a(f) - 2S_{VAC}(f) \otimes S_{VAC}(f) + 4S_s(f) \otimes S_a(f). \quad (3)$$

B. Fiber Link Model

A lossy optical fiber is modeled [Fig. 1(c)] as a beamsplitter with a transmittance $a < 1$ equal to the power attenuation of the fiber, and a reflective input port open to the vacuum field, adding noise to the signal. In terms of power, we have the block scheme shown in Fig. 1(d) and get the output power spectral density as

$$S_{OUT} = aS_{IN} + (1 - a)S_{VAC} \quad (4)$$

The model exactly accounts for signal and noise of a field propagating down a fiber of length L which attenuates the power by a factor $a = 10^{-\alpha L/10}$.

III. LINKS WITH EDFA REGENERATION

We can now apply the models described in Section II to calculate signal and noise of optical links with OA's. We allow for amplifier saturation by means of a simple phenomenological description [2], by letting the active fiber gain as

$$g(\lambda_{in}) = g_0(\lambda_{in}) / (1 + \overline{P_{AMP}} / P_{sat}) \quad (5)$$

where g_0 is the unsaturated gain per length unit, $\overline{P_{AMP}} = P_{in}(e^{gL_{EDF}} - 1) / gL_{EDF}$ is the average power along the active fiber, L_{EDF} is the erbium doped fiber length, $P_{in} = P_s + P_{ASE}$ is the total input power given by the sum of the input ASE and the signal, P_{sat} is the OA saturation power and λ_{in} is the wavelength of the saturating input (i.e., the signal wavelength

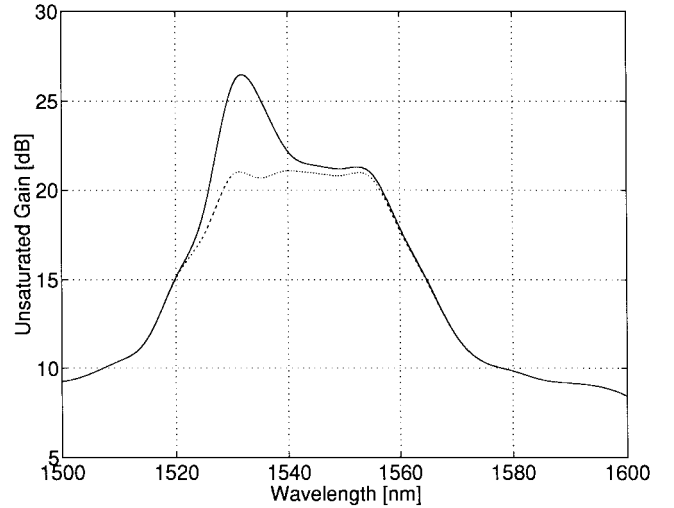


Fig. 2. Gain of the OA assumed in the calculation. Solid line: EDFA without filter; dotted line: EDFA with gain flattening filter.

if $P_s > P_{ASE}$, the ASE peak wavelength if $P_{ASE} > P_s$). The unsaturated gain is then:

$$g_0(\lambda) = [\sigma_e(\lambda)N_{e,0} - \sigma_a(\lambda)N_{a,0}]L_{EDF} \quad (6)$$

where σ_e and σ_a are the emission and absorption cross section of the doped fiber, $N_{e,0}$ and $N_{a,0}$ are the unsaturated ion population of the metastable and ground level. Values used in the calculations are $N_{e,0} = 0.68 \cdot 10^{18}$ ions/cm³ and $N_{a,0} = 0.12 \cdot 10^{18}$ ions/cm³, $P_{sat} = 3.6$ mW for an OA length of 20 m. From (5), we obtain the saturated gain $g(\lambda_{in})$, and calculate N_e and N_a by an equation similar to (6). Then we find the saturated gain $G(\lambda) = e^{[\sigma_e(\lambda)N_e - \sigma_a(\lambda)N_a]L_{EDF}}$ and the spontaneous emission coefficient

$$N_{sp}(\lambda) = \sigma_e(\lambda)N_e / [\sigma_e(\lambda)N_e - \sigma_a(\lambda)N_a]. \quad (7)$$

We have considered an EDFA made of 20 m fluorine-phosphate glass fiber, whose unsaturated gain has a marked peak around 1530 nm [2], see Fig. 2, full line. To study the ASE evolution, we simulated 100 concatenated OA's with 60 km spacing, with no input signal and no filtering. Fig. 3 shows the spectral density of the ASE after 10, 50, 100 OA's. This model correctly describes the self-filtering effect, experimentally reported in [13], that enhances the 1550 nm peak and flattens the 1530 nm one, due to the spectral change of the saturated gain. We have also repeated the same calculation for an OA gain-flattened with passive filters. The equalized gain shape shown in Fig. 2 (dotted line) is actually employed in a prototype OA [14]. Interesting to note, the result still exhibits the self-filtering action (see Fig. 3, dotted line) after a certain number of cascaded OA's.

IV. PARAMETRIC GAIN AND FIBER LINK NOISE

Fiber nonlinearities can be included in our model by means of the well-known description of propagation based on the nonlinear Schrödinger equation, that we write here explicitly to define used terms [5]

$$\frac{\partial U}{\partial z} = -\frac{1}{2}\alpha U - \frac{i}{2}\beta_2 \frac{\partial^2 U}{\partial T^2} + i\gamma|U|^2 U \quad (8)$$

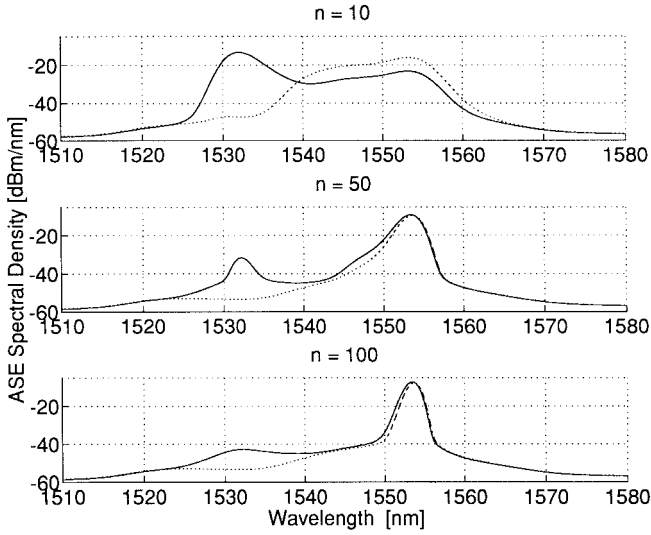


Fig. 3. ASE spectral density after 10, 50, 100 EDFA's, showing the ASE self-filtering effect. $\alpha = 0.2$ dB/km, no input signal, distance between OA's: 60 km. Solid line: EDFA without filter; dotted line: EDFA with gain flattening filter.

where U is the electric field, T is the retarded time frame, α is the power attenuation coefficient, β_2 is the fiber dispersion parameter and γ is the nonlinear coefficient of the fiber. The stationary solution for a signal with power P_0 is of the type

$$U(z, T) = \sqrt{P_0} e^{-(\alpha/2)z} e^{i(\omega_0 T - \Phi_{NL})} \quad (9)$$

$\Phi_{NL} = \gamma P_0 \int_0^z e^{-\alpha\zeta} d\zeta$ being the nonlinear phase.

The nonlinear effect on the noise field is treated by adding a probe $a(z, T)$ to the signal, in the form of small perturbation

$$U(z, T) = (\sqrt{P_0} + a(z, T)) e^{-(\alpha/2)z} e^{i(\omega_0 T - \Phi_{NL})}. \quad (10)$$

By substituting (10) in (8) and linearizing on a we get

$$\frac{\partial a}{\partial z} = -\frac{i}{2} \beta_2 \frac{\partial^2 a}{\partial T^2} + i\gamma P_0 e^{-\alpha z} 2 \operatorname{Re}(a) \quad (11)$$

where the real part of a is the component of a in phase with the signal. Then we obtain for the Fourier transform of the real and imaginary part of a

$$\begin{aligned} \frac{\partial A_r(z, \Omega)}{\partial z} &= \frac{1}{2} \beta_2 \Omega^2 A_i(z, \Omega) \\ \frac{\partial A_i(z, \Omega)}{\partial z} &= -\frac{1}{2} \beta_2 \Omega^2 A_r(z, \Omega) \\ &\quad - 2\gamma P_0 e^{-\alpha z} A_r(z, \Omega) \end{aligned} \quad (12)$$

where the subscript r indicates the real part and i the imaginary, and Ω is the difference between noise and signal frequency. An analytical solution can be found in matrix form [7] using the approximation of constant signal power along the fiber of length L (equal to its path-averaged value $\bar{P} = P_0(1 - e^{-\alpha L})/\alpha L$)

$$\begin{bmatrix} A_r(z, \Omega) \\ A_i(z, \Omega) \end{bmatrix} = H(z, \Omega) \begin{bmatrix} A_r(0, \Omega) \\ A_i(0, \Omega) \end{bmatrix} \quad (13)$$

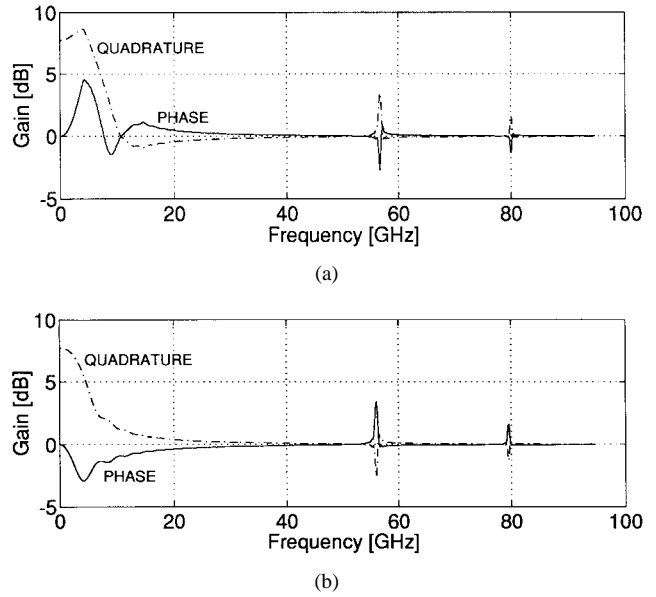


Fig. 4. (a) Parametric Gain experienced by the probe signal in the anomalous dispersion regime. Fiber link length: 2500 km; amplifier spacing: 50 km; signal power 1 mW after each OA; $\beta_2 = -1$ ps²/km; $\alpha = 0.22$ dB/km; $\gamma = 2$ W⁻¹ km⁻¹. (b) The same in normal dispersion regime ($\beta_2 = +1$ ps²/km).

where

$$H(z, \Omega) = \begin{bmatrix} \cos(kz) & -\xi \sin(kz) \\ \xi^{-1} \sin(kz) & \cos(kz) \end{bmatrix} \quad (14)$$

$$\xi = \left(\frac{\frac{1}{2} \beta_2 \Omega^2}{\frac{1}{2} \beta_2 \Omega^2 + 2\gamma \bar{P}} \right)^{1/2} \quad (15)$$

$$k = \sqrt{\frac{1}{2} \beta_2 \Omega^2 (\frac{1}{2} \beta_2 \Omega^2 + 2\gamma \bar{P})}. \quad (16)$$

The power spectrum matrix of a is the Fourier transform of the autocorrelation and cross-correlation functions $\Re(\tau)$ between the real and imaginary part of a , i.e.

$$\Sigma(z, \Omega) = \begin{bmatrix} F(\Re_{ar-ar}(\tau)) & F(\Re_{ar-ai}(\tau)) \\ F(\Re_{ai-ar}(\tau)) & F(\Re_{ai-ai}(\tau)) \end{bmatrix}. \quad (17)$$

The transmission law for the power spectrum matrix due to nonlinear effects is then

$$\Sigma'(z, \Omega) = H(z, \Omega) \Sigma(0, \Omega) H^T(z, \Omega) e^{-\alpha z} \quad (18)$$

where the fiber attenuation has also been included.

To calculate the evolution of the power spectral density, the link is divided into spans short enough to have the signal power P_0 nearly constant in it (i.e., it shall be $\alpha z \ll 1$). The calculation for the interaction between the signal and the perturbative probe field holds under the approximation of undepleted signal. To take into account the exchanged power, we subtract from the signal the power accumulated by the probe at the end of each span.

Fig. 4 shows the PG of the in phase and quadrature components of the probe signal, for a 2500-km fiber link, with 50-km amplifier span, in anomalous and normal dispersion. Because of the segmentation of the link, the results are in qualitative agreement but slightly different from those found in [7]; in particular, the in-phase peak for the anomalous dispersion

regime is reduced. The peaks at 57 and 80 GHz, known as sideband instability effect [15], are due to the periodic variation of the signal power that acts as a sort of phase-grating. If the OA spacing is randomly changed by 10%, the peak structure damps out, however still at constant total power. The sideband instability effect can be detrimental for multiwavelength transmission systems, because it introduces crosstalk.

A. Effect of Vacuum Noise

In our model we explicitly incorporate the noise contribution of the vacuum field entering the transmission link at lossy devices, i.e., fiber, splices, connectors, filters (see Section II-B). This noise contribution accounts for SNR degradation of an unamplified signal [1]; after signal amplification, the vacuum noise term becomes generally negligible, and the excess noise from OA's (i.e., the ASE) becomes the dominant noise source.

To analyze the effect of the vacuum field noise in presence of nonlinear gain, we evaluate the vacuum field contribution introduced by the attenuation in a nonlinear fiber span. Let us consider an elemental fiber section Δz at z and its attenuation $e^{-\alpha\Delta z}$. The additional noise power due to the vacuum field is $(1 - e^{-\alpha\Delta z})S_{\text{VAC}}$, and the noise term generated at z undergoes both the nonlinear PG interaction and the attenuation from that point to the end of the link of length L , yielding an output noise power given by

$$\begin{aligned} \Delta S_{\text{PG,VAC},z}(L) &= (1 - e^{-\alpha\Delta z}) \cdot H_z(L - z, \Omega) \cdot \Sigma_{\text{VAC}}(\Omega) \\ &\quad \cdot H_z^T(L - z, \Omega) e^{-\alpha(L-z)} \end{aligned} \quad (19)$$

where $H_z(L - z, \Omega)$ is given by (14)–(16), represents the signal power averaged on the span $[z, L]$ and

$$\Sigma_{\text{VAC}}(\Omega) = \begin{bmatrix} \frac{1}{4}h\nu & 0 \\ 0 & \frac{1}{4}h\nu \end{bmatrix}. \quad (20)$$

All the contributions of the kind (19) generated from 0 to L coordinate are uncorrelated, and add up to give the total output noise as

$$\begin{aligned} S_{\text{PG,VAC,TOT}}(L) &= \sum_{L/\Delta z} \Delta S_{\text{PG,VAC},z}(L) \\ &= \sum_{n=1}^{L/\Delta z} (1 - e^{-\alpha\Delta z}) \cdot \Sigma_{\text{VAC}}(\Omega) \cdot e^{-\alpha(L-n\Delta z)} \\ &\quad \cdot H_{n\Delta z}(L - n\Delta z, \Omega) H_{n\Delta z}^T(L - n\Delta z, \Omega) \\ &\cong \sum_{n=1}^{L/\Delta z} \alpha\Delta z \cdot \Sigma_{\text{VAC}}(\Omega) \cdot e^{-\alpha(L-n\Delta z)} \\ &\quad \cdot H_{n\Delta z}(L - n\Delta z, \Omega) H_{n\Delta z}^T(L - n\Delta z, \Omega) \\ &\xrightarrow{\Delta z \rightarrow 0} \int_0^L \alpha \cdot \Sigma_{\text{VAC}}(\Omega) \cdot e^{-\alpha(L-z)} \\ &\quad \cdot H_z(L - z, \Omega) H_z^T(L - z, \Omega) dz. \end{aligned} \quad (21)$$

The above expression gives the total noise contribution due to vacuum field that must be added to (18).

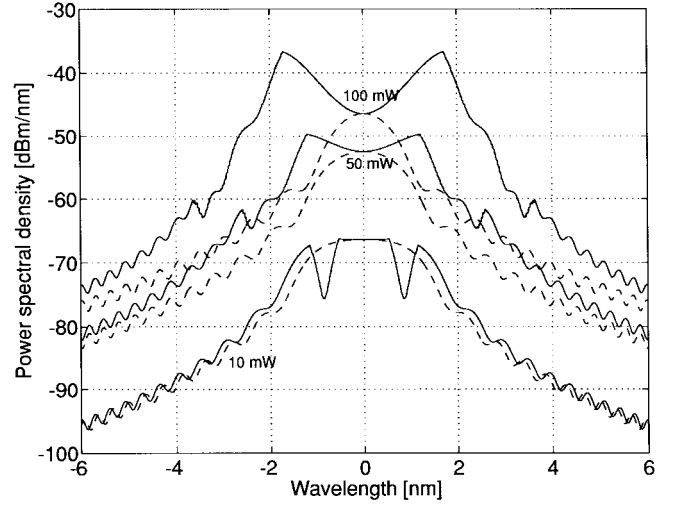


Fig. 5. Optical measurable spectra at the end of 30 km fiber without OA's, showing vacuum field amplification by PG. Signal wavelength: 1550 nm; signal power: 10, 50, 100 mW; $\beta_2 = +0.1$ ps²/km (dashed line) and $\beta_2 = -0.1$ ps²/km (solid line). The signal is not shown.

It is possible to give a simpler approximate expression for the noise spectral density (21), exploiting the link segmentation as previously done. The fiber attenuation is lumped at the end of each span and, according to Section II, this attenuation opens a port to the vacuum field, so the power spectrum matrix after the span of length z is

$$\begin{aligned} \Sigma(z, \Omega) &= H(z, \Omega) \Sigma(0, \Omega) H^T(z, \Omega) \cdot e^{-\alpha z} \\ &\quad + (1 - e^{-\alpha z}) \Sigma_{\text{VAC}}(\Omega). \end{aligned} \quad (22)$$

This model converges to the exact solution (21) for the condition $\alpha z \ll 1$, and has been used instead of (21) to simplify the calculation.

To evaluate the enhancement of the vacuum noise field due to PG when (21) is the dominant noise term, let us consider a 1550 nm coherent light signal (i.e., with no ASE excess noise [1]) and calculate the spectrum of the optical field at the end of a purely passive nonlinear fiber link. The measurable optical noise spectrum, calculated as the difference between the total output spectrum and the vacuum field spectrum [1], is shown in Fig. 5. The spectrum is obtained after 30 km of fiber for different laser powers and for anomalous and normal dispersion fiber ($\beta_2 = -0.1$ ps²/km and $\beta_2 = +0.1$ ps²/km), and it exhibits a remarkable power exchange from signal to noise field.

The results show that PG can really act on the vacuum field, and hence this effect shall be taken into account in the evaluation of optical link noise. As an example, we calculate the SNR degradation along an optically amplified fiber link with and without the effect of vacuum noise. The detailed calculation of the detected electrical SNR evolution along the link is reported in the Appendix. The link, shown in the inset of Fig. 6 consists of a 20 mW 1550 nm laser and six 50 km conventional fiber spans interposed by 5 OA's of 26.7 m length (at the output of each OA the power is 20 mW). Fig. 6(a) reports SNR degradation for three cases: an ideal linear fiber (dash-dotted line); a nonlinear fiber neglecting vacuum contribution (dashed line) and a nonlinear

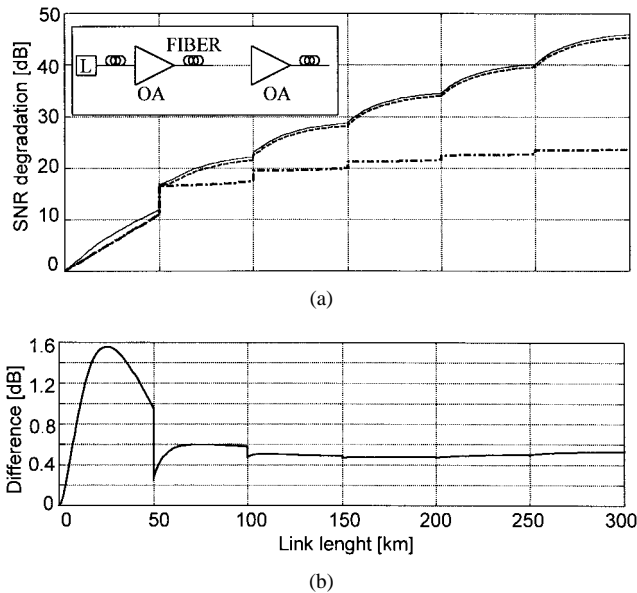


Fig. 6. (a) SNR degradation of a 20 mW 1555 nm signal along 300-km fiber link with 5 OA's ($\beta_2 = -20$ ps²/km; $\alpha = 0.22$ dB/km; $\gamma = 2$ W⁻¹ km⁻¹; electrical filter bandwidth: 5 GHz). Dash-dotted line: absence of nonlinear effects; dashed line: no vacuum noise contribution; solid line: vacuum noise contribution taken into account. (b) Difference between the two latter cases, showing SNR degradation enhancement due to vacuum field parametric amplification.

fiber taking parametric amplification of vacuum field into account. Fig. 6(b) shows the difference between the two latter cases: this is the contribution of the vacuum noise. The effect of nonlinear vacuum field amplification is remarkable at the beginning of the link, it decreases abruptly after the first OA due to the ASE, it increases again along the second fiber span, than it becomes almost constant: still at the end of the link a 0.5 dB SNR difference is observed.

V. ANALYSIS OF TRANSMISSION LINKS

We now apply the noise model described in previous sections to transmission fiber link with OA's, including dispersion, nonlinear effects and vacuum contribution. Long- and short-haul links are chosen as examples to validate the proposed noise model. Signal to noise ratio and overall noise figure are calculated rather than bit error rate, because of the nonwhite noise coming from PG (no simple formulas) and also because a more complicated description taking into account the bit pattern and self-phase modulation is needed [12].

A. Long-Haul Amplified Systems

First, we consider a 2500-km link in anomalous dispersion regime ($\beta_2 = -1$ ps²/km, $\gamma = 2$ W⁻¹ km⁻¹, $\alpha = 0.22$ dB/km), amplified by 50 equally spaced 16.5-m long EDFA's (the 1 mW 1555 nm laser is followed by a booster-OA and by 50 fiber span interposed by 49 OA's). After each OA, we put an optical filter with Lorentzian shape and FWHM of 8 nm, in order to avoid EDFA saturation by ASE amplification.

Fig. 7 shows the optical spectral density at the end of the link, compared with the ASE after the first amplifier. Fig. 8 is

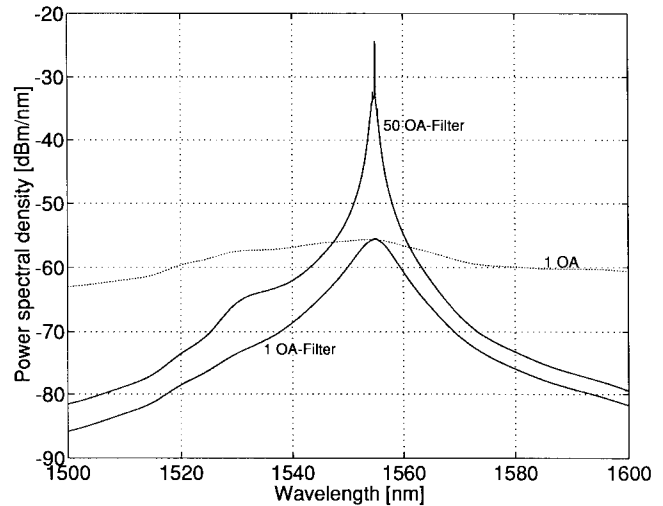


Fig. 7. Optical spectrum at the output of a long-span link (2500 km) with 50 OA's (solid line), compared with the spectrum after 1 OA (50 km link) with and without (dotted line) filter. Signal wavelength 1555 nm; signal input power 1 mW.

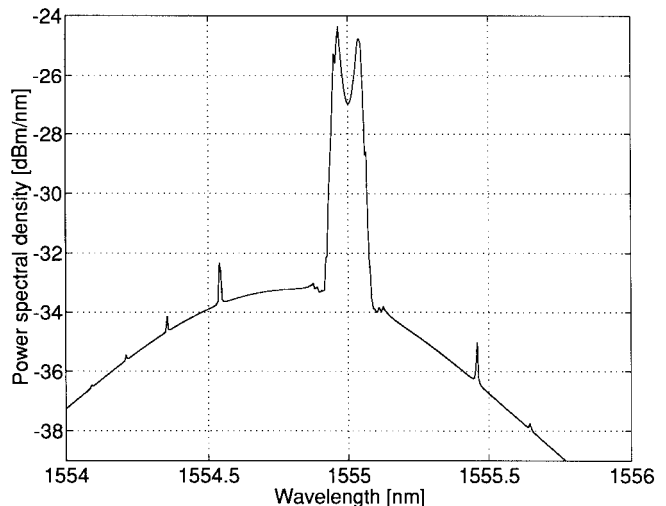


Fig. 8. As in Fig. 6 but with expanded scale to show the effect of PG.

a zoom of Fig. 7 that shows the effect of PG which yields 8 dB gain in a bandwidth of about 10 GHz. Note the sideband peaks 0.46 nm (57 GHz) away from the signal wavelength.

Fig. 9 shows the SNR evolution for a 5 GHz electrical bandwidth in fibers with different dispersion values, compared with that of an ideal linear link. The simulation is also performed for the same 2500 km link regenerated by 25 and 83 EDFA's, respectively, 23 and 14.2 m long, with 100 and 30 km repeater spacing. All the systems are designed to have 1 mW signal at the output of each OA, to compare their performances given one fixed parameter. In all cases, the link performance worsens for low dispersion values: this is due to the increase of the PG bandwidth as the inverse square root of β_2 .

B. Short Distance Systems

As representative of a intercity connection, we consider a transmission link of 120 km standard SM fiber with $\beta_2 = -20$

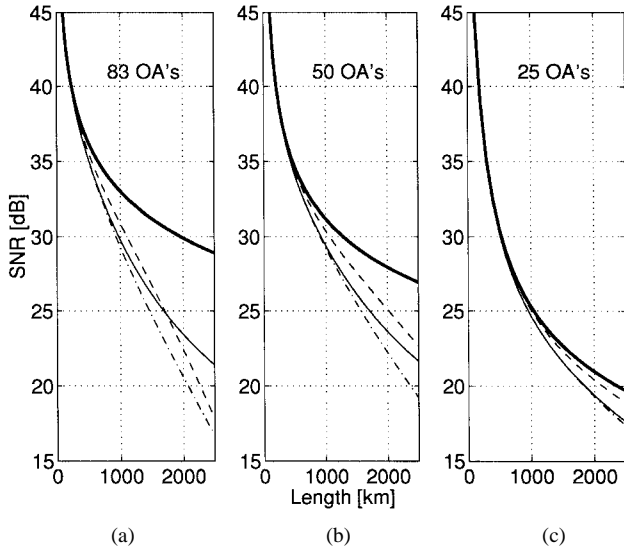


Fig. 9. SNR evolution along a 2500-km link for different OA's spacing: absence of nonlinear effects (thick line), fiber with $\beta_2 = -20 \text{ ps}^2/\text{km}$ (dashed line), $\beta_2 = -1 \text{ ps}^2/\text{km}$ (dash-dotted line), $\beta_2 = +1 \text{ ps}^2/\text{km}$ (solid line). OA's spacing: (a) 30 km, (b) 50 km, and (c) 100 km. Electrical filter bandwidth: 5 GHz.

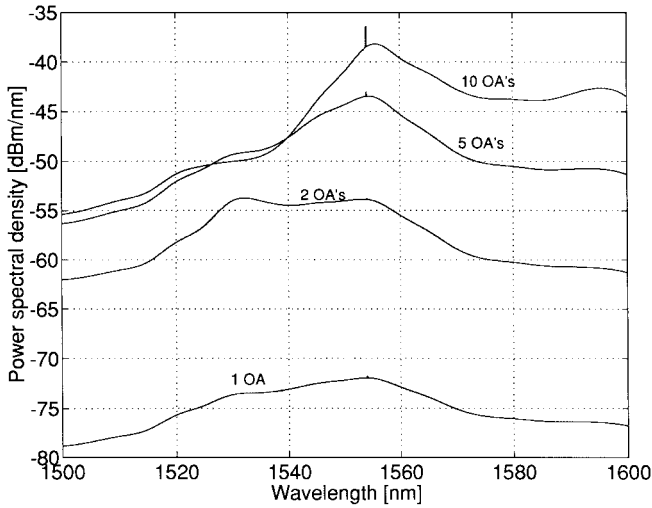


Fig. 10. Optical spectrum at the output of 120 km link with 1, 2, 5, 10 OA's. Signal wavelength 1554 nm, input signal power 1 mW, $\beta_2 = -20 \text{ ps}^2/\text{km}$.

ps^2/km , $\gamma = 2 \text{ W}^{-1} \text{ km}^{-1}$ and $\gamma = 0.22 \text{ dB/km}$. The input of the booster-OA is a 1 mW, 1554 nm signal.

An unfiltered link with OA's has the output optical spectra of Fig. 10, for 1, 2, 5, and 10 OA's. All the OA's are 15 m long. It is interesting to note the shift of the ASE peak to longer wavelength with increasing OA's number (for long and deeply saturated amplifiers the gain always moves to longer wavelengths, with substantial amplification up to 1620 nm). The noise figure evolution along the link is shown in Fig. 11; from here we can see that a link with 10 OA's is worse than one with 5 due to the enhancement of PG caused by the larger signal power.

To investigate the optimum OA's number, we calculate the NF of the 120 km link as a function of the OA number and

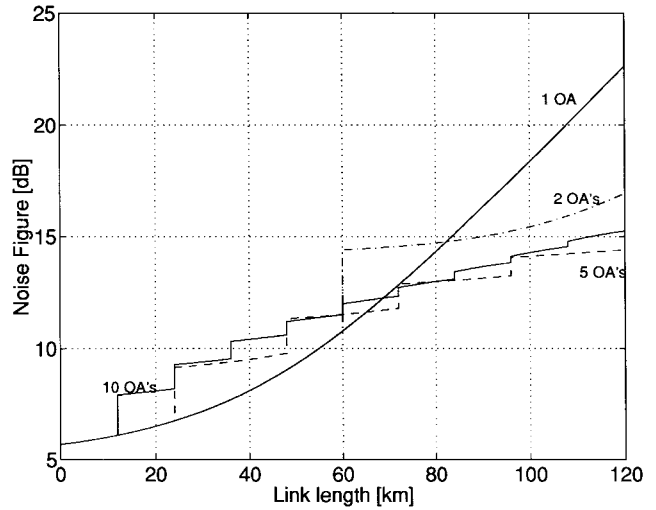


Fig. 11. Noise figure evolution along the 120 km link for varying OA's number. 1 mW input signal power at 1554 nm, $\beta_2 = -20 \text{ ps}^2/\text{km}$, electrical filter bandwidth: 5 GHz.

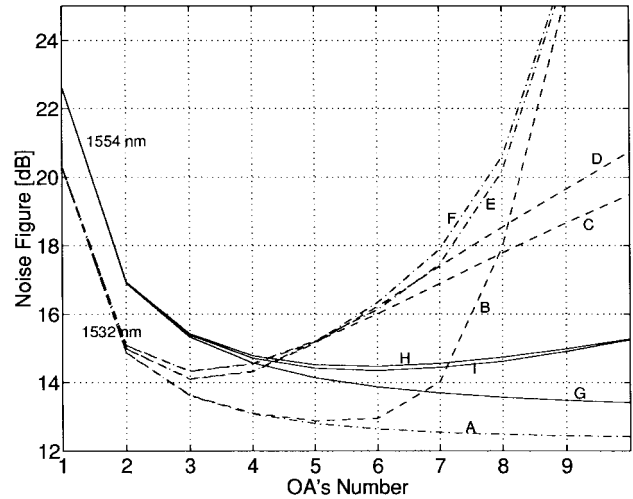


Fig. 12. Noise figure of a 120-km link as a function of the OA's number, for different signal wavelengths and fiber dispersion coefficients. (a) 1532 nm, optically filtered, linear case, (b) 1532 nm, unfiltered linear case, (c) 1532 nm, optically filtered, $\beta_2 = -1 \text{ ps}^2/\text{km}$, (d) 1532 nm, optically filtered, $\beta_2 = -20 \text{ ps}^2/\text{km}$, (e) 1532 nm, unfiltered, $\beta_2 = -1 \text{ ps}^2/\text{km}$; (f) 1532 nm, unfiltered, $\beta_2 = -20 \text{ ps}^2/\text{km}$; (g) 1554 nm, unfiltered, linear case; (h) 1554 nm, unfiltered, $\beta_2 = -1 \text{ ps}^2/\text{km}$; (i) 1554 nm, unfiltered, $\beta_2 = -20 \text{ ps}^2/\text{km}$. The optical filter has a Lorentzian shape with 8 nm FWHM.

the results are plotted in Fig. 12. In the linear case the curve is monotone for 1554 nm signal, while at 1532 nm it shows a sharp increase after 6 OA's because of saturation by ASE amplification, that can be reduced by filtering (with the 8 nm filter). As nonlinear effects are taken into account, the curve always exhibits a minimum, found at 1554 nm for six OA's and at 1532 nm for three OA's (unsaturated gain is higher in the second case).

Interesting to note, after a certain number of amplifiers, the system works better with $\beta_2 = -1 \text{ ps}^2/\text{km}$ than with $\beta_2 = -20 \text{ ps}^2/\text{km}$, even if the power exchanged by PG decreases with the absolute value of β_2 . This is due to the 5 GHz receiver

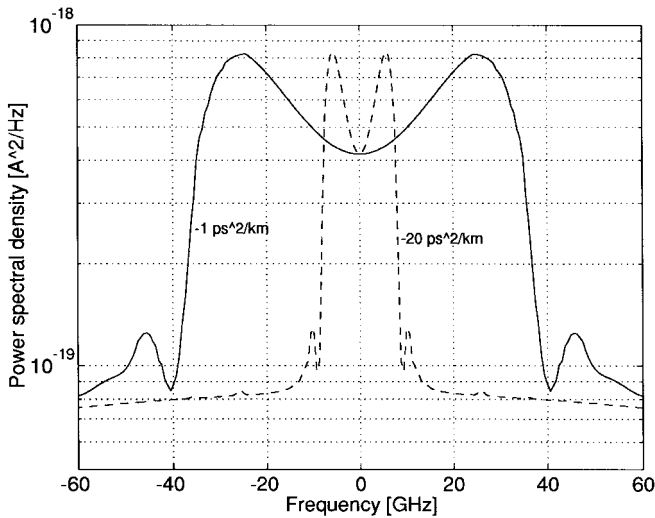


Fig. 13. Power spectral density of the photocurrent noise, detected after a 120 km fiber link with 10 OA's. Input signal wavelength 1532 nm, power 1 mW, $\beta_2 = -20$ ps²/km (dashed line), $\beta_2 = -1$ ps²/km (solid line).

electrical filter (0.04 nm at 1532 nm) that cuts the electrical noise peak induced by PG (see Fig. 13).

VI. CONCLUSION

In this paper, we have shown that a semiclassical noise model for the OA can be easily extended to incorporate fiber noise, OA saturation, dispersion and nonlinear interaction, so as to treat transmission links with cascaded OA's. Results of calculations for long-haul link and intercity connection have been presented, which confirm the importance of nonlinear effects to determine the optimal link structure. A general agreement with previously formal results is obtained by our approach which is straightforward and self-consistent. We have also considered the nonlinear interaction between signal and vacuum field which, to our knowledge, has never been pointed out previously. Numerical evaluation of this effect shows that it can be of importance in some practical cases, e.g., for a coherent signal on a short link.

APPENDIX

Let us consider a photodiode with an impinging optical field $E(t)$. The photocurrent is

$$I(t) = \frac{e}{h\nu} |E(t)|^2. \quad (23)$$

The field $E(t)$ is made up by the signal and an additive noise $a(t, z)$

$$E(t) = [s(t) + a(t)] e^{j(\omega_0 t - \Phi_{NL})}. \quad (24)$$

Neglecting multiplicative constants the current is worth

$$I(t) = s^2(t) + a^2(t) + 2s(t)a(t). \quad (25)$$

Let us calculate the current autocorrelation function (underlined terms are zero-mean) [16]

$$\begin{aligned} \mathfrak{R}_r(\tau) &= \langle (s^2(t) + a^2(t) + 2s(t)a(t))(s^2(t-\tau) \\ &\quad + a^2(t-\tau) + 2s(t-\tau)a(t-\tau)) \rangle \\ &= \langle s^2(t)s^2(t-\tau) \rangle + \langle a^2(t)a^2(t-\tau) \rangle \\ &\quad + \langle 2s(t)a(t)2s(t-\tau)a(t-\tau) \rangle + \langle s^2(t)a^2(t-\tau) \rangle \\ &\quad + \langle s^2(t)2s(t-\tau)a(t-\tau) \rangle + \langle a^2(t)s^2(t-\tau) \rangle \\ &\quad + \langle a^2(t)2s(t-\tau)a(t-\tau) \rangle + \langle 2s(t)a(t)s^2(t-\tau) \rangle \\ &\quad + \langle 2s(t)a(t)a^2(t-\tau) \rangle \\ &= \langle s^2(t)s^2(t-\tau) \rangle + \langle a^2(t)a^2(t-\tau) \rangle \\ &\quad + 4\langle s(t)s(t-\tau) \rangle \langle a(t)a(t-\tau) \rangle \\ &\quad + \langle s^2(t) \rangle \langle a^2(t-\tau) \rangle + \langle s^2(t)2s(t-\tau) \rangle \langle a(t-\tau) \rangle \\ &\quad + \langle a^2(t) \rangle \langle s^2(t-\tau) \rangle + \langle a^2(t)a(t-\tau) \rangle \langle 2s(t-\tau) \rangle \\ &\quad + \langle 2s(t)s^2(t-\tau) \rangle \langle a(t) \rangle + \langle 2s(t) \rangle \langle a(t)a^2(t-\tau) \rangle \\ &= \mathfrak{R}_{s^2}(\tau) + \mathfrak{R}_{a^2}(\tau) + 4\mathfrak{R}_s(\tau)\mathfrak{R}_a(\tau) \\ &\quad + 2\mathfrak{R}_s(0)\mathfrak{R}_{a_r}(0). \end{aligned} \quad (26)$$

The above terms yield (s is a deterministic signal of power P_s and a is a Gaussian stochastic variable) [16]

$$\mathfrak{R}_{s^2}(\tau) = \langle s^2(t)s^2(t-\tau) \rangle = P_s^2 = \mathfrak{R}_s^2(0) \quad (27)$$

$$\begin{aligned} \mathfrak{R}_{a^2}(\tau) &= \langle a^2(t)a^2(t-\tau) \rangle \\ &= \langle a^2(t) \rangle \langle a^2(t-\tau) \rangle + 2\langle a(t)a(t-\tau) \rangle^2 \\ &= \mathfrak{R}_a^2(0) + 2\mathfrak{R}_a^2(\tau). \end{aligned} \quad (28)$$

The current power spectral density is formally given by Fourier transform of the autocorrelation

$$\begin{aligned} S_i(f) &= F\{\mathfrak{R}_r(\tau)\} = \left[\int_{-\infty}^{+\infty} (S_s(f) + S_a(f)) df \right]^2 \delta(f) \\ &\quad + 2S_a(f) \otimes S_a(f) + 4S_s(f) \otimes S_a(f). \end{aligned} \quad (29)$$

The first term in (29) is the received continuous wave (CW) power, the second is known in literature as noise-noise beating and the third as signal-noise beating. Note from (24) that the noise a is considered baseband.

If we consider the power spectrum matrix

$$\Sigma(f) = \begin{bmatrix} S_{a_r}(f) & s_{a_{ri}}(f) \\ S_{a_{ir}}(f) & S_{a_i}(f) \end{bmatrix} \quad (30)$$

the noise spectral density is worth

$$S_a(f) = \frac{1}{2} [S_{a_r}(f) + S_{a_i}(f)] \quad (31)$$

because the direct detection averages phase and quadrature fluctuations.

At last the vacuum field contribution shall be subtracted from the photocurrent [1]

$$\begin{aligned} S_i(f) &= \left[\int_{-\infty}^{+\infty} (S_s(f) + S_a(f) - S_{\text{VAC}}(f)) df \right]^2 \delta(f) \\ &\quad + 2S_a(f) \otimes S_a(f) - 2S_{\text{VAC}}(f) \otimes S_{\text{VAC}}(f) \\ &\quad + 4S_s(f) \otimes S_a(f) \end{aligned} \quad (32)$$

indeed, the energy exchanged in the matter-radiation interaction is the difference between the excited-state energy and the

ground state (i.e., the vacuum field) energy of the radiation. By (32) it is easy to calculate the noise of the photocurrent as a function of the input electromagnetic field.

REFERENCES

- [1] S. Donati and G. Giuliani, "Noise in an optical amplifier: Formulation of a new semiclassical model," *IEEE J. Quantum Electron.*, vol. 33, pp. 1481–1488, Aug. 1997.
- [2] E. Desurvire, *Erbium-Doped Fiber Amplifiers-Principle and Applications*. New York: Wiley, 1994.
- [3] N. A. Olsson, "Lightwave systems with optical amplifiers," *J. Lightwave Technol.*, vol. 7, pp. 1071–1082, 1989.
- [4] E. Berglind and L. Gillner, "Optical quantum noise treated with classical electrical network theory," *IEEE J. Quantum Electron.*, vol. 30, pp. 846–853, 1994.
- [5] G. P. Agrawal, *Nonlinear Fiber Optics*. New York: Academic, 1989.
- [6] M. Yu, G. P. Agrawal, and C. J. McKinstrie, "Pump-wave effects on the propagation of noisy signals in nonlinear dispersive media," *J. Opt. Soc. Amer. B*, vol. 12, pp. 1126–1132, 1995.
- [7] C. Lorattanasane and K. Kikuchi, "Parametric instability of optical amplifier noise in long-distance optical transmission systems," *IEEE J. Quantum Electron.*, vol. 33, pp. 1068–1074, July 1997.
- [8] A. Carena, V. Curri, R. Gaudino, P. Poggiolini, and S. Benedetto, "New analytical result on fiber parametric gain and its effects on ASE noise," *IEEE Photon. Technol. Lett.*, vol. 9, pp. 535–537, Apr. 1997.
- [9] A. Mecozzi, "Long-distance transmission at zero dispersion: Combined effect of the Kerr nonlinearity and the noise of the in-line amplifiers," *J. Opt. Soc. Amer. B*, vol. 11, pp. 462–469, 1994.
- [10] M. O. van Deventer, S. Wingstrand, B. Hermansson, A. Bolle, P. Jalderot, C. Backdahl, and J. Karlsson, "BER floor due to modulation instability in a 2.5 Gbit/s field trial with +22 dBm booster EDFA," *Optical Fiber Technol.*, vol. 2, pp. 183–188, 1996.
- [11] R. Hui, M. O'Sullivan, A. Robinson, and M. Taylor, "Modulation instability and its impact in multispan optical amplified IMDD systems: Theory and experiments," *J. Lightwave Technol.*, vol. 15, pp. 1071–1081, 1997.
- [12] F. Matera and M. Settembre, "Exploitation of the fiber capacity in optically amplified transmission systems," *Optical Fiber Technol.*, vol. 4, pp. 34–82, 1998.
- [13] B. M. Desthieux, M. Suyama, and T. Chikama, "Theoretical and experimental study of self-filtering effect in concatenated erbium-doped fiber amplifiers," *J. Lightwave Technol.*, vol. 12, pp. 1405–1411, Aug. 1994.
- [14] L. Boschis, L. Cognolato, A. Pagano, M. Potenza, O. Rossotto, B. Sordo, and L. Tallone, "Three uniform long-period grating for 1-dB gain flattened EDFA," in *Proc. LEOS Workshop Fiber Optic Passive Components'98, WFOPC'98*, Pavia, Italy, Sept. 1998, pp. 11–15.
- [15] F. Matera, A. Mecozzi, M. Romagnoli, and M. Settembre, "Sideband instability induced by periodic power variation in long-distance fiber links," *Opt. Lett.*, vol. 18, pp. 1499–1501, Sept. 1993.
- [16] A. Papoulis, *Probability, Random Variables, and Stochastic Processes*, 3rd ed. New York: McGraw-Hill, 1991.

Michele Norgia (S'99) was born in Omegna, Italy, in 1972. He received the degree with Honors in electronics engineering from the University of Pavia, Pavia, Italy, in 1996 with a thesis on noise in optical amplifiers. He is currently pursuing the Ph.D. degree in electronics engineering and computer science at the University of Pavia, working in the Optoelectronics group.

His main research interests are noise in optical amplifiers and interferometry.

Guido Giuliani (M'99) was born in Milan, Italy, in 1969. He received the degree with honors in electronic engineering from University of Pavia, Pavia, Italy, in 1993 and the Ph.D. degree in electronics and computer science from the same University in 1997.

He is now Postdoctoral Researcher at the Dipartimento di Elettronica, University of Pavia. His main research interests are diode laser feedback interferometry, optical amplifier noise, semiconductor optical amplifiers, and electrooptical gyroscopes.

Silvano Donati (M'75–SM'98) was born in Milan, Italy, on August 19, 1942 and received the degree in physics cum laude at the University of Milan in 1966.

From 1966 to 1975, he was with CISE (Milan), carrying out research on noise in photomultipliers and avalanche photodiodes, nuclear electronics and electrooptic instrumentation. In 1975, he joined the Department of Electronics, University of Pavia, Italy, where he became full Professor of Optoelectronics in 1980. He has worked on laser interferometry, fiber gyroscopes and noise in CCD's and, more recently, on optical fiber sensors, passive fiber components for telecommunications, and optical interconnections. He has authored or coauthored about 160 papers and holds eight patents. He is the author of the book, *Photodetectors* (Englewood Cliffs, NJ, Prentice Hall, 1999).

Mr. Donati is a Meritorious Member of AEI, and member of the APS, OSA, ISHM, and has served to organize several national and international meetings (WFOPC, ODIMAP) and schools as a Chairman or in steering and programme committees. He has founded and is the present Chair of the Italian LEOS.